

Probing nuclear structure using elliptic flow of strange and multi-strange hadrons in isobar collisions

Priyanshi Sinha (for the STAR collaboration)^{1*}

¹Indian Institute of Science Education and Research (IISER) Tirupati

*priyanshisinha@students.iisertirupati.ac.in

July 11, 2023

Abstract

The data for isobar collisions ($^{96}\text{Ru}+^{96}\text{Ru}$ and $^{96}\text{Zr}+^{96}\text{Zr}$) at $\sqrt{s_{\text{NN}}} = 200$ GeV has been taken at RHIC in the year 2018. The elliptic flow (v_2) for charged hadrons differs in the two isobar collision systems, which indicates a difference in the nuclear structure between the two nuclei. We report the transverse momentum (p_T) and centrality dependence of v_2 of K_s^0 , Λ , $\bar{\Lambda}$, ϕ , Ξ^- , and $\bar{\Xi}^+$ particles at mid-rapidity for Ru+Ru and Zr+Zr collisions at $\sqrt{s_{\text{NN}}} = 200$ GeV. We also compare the results to those in Cu+Cu, Au+Au, and U+U collisions to understand the system size dependence.

1 Introduction

Heavy-ion collisions at the Relativistic Heavy Ion Collider (RHIC) and Large Hadron Collider (LHC) indicates the presence of a strongly interacting medium called Quark Gluon Plasma (QGP). Elliptic flow studies of the produced particles in this medium provide an understanding the early time anisotropy in the medium. In 2018, a dedicated isobar collision run of Ru+Ru and Zr+Zr $\sqrt{s_{\text{NN}}} = 200$ GeV was successfully

23 carried out at RHIC. Despite the same nucleon number, the anisotropic flow coeffi-
 24 cients were observed to be different in the two collision systems [1]. This indicates
 25 that the difference in nuclear structure may also leave imprints on the elliptic flow
 26 of particles. Recent studies also discuss probing of nuclear structures via v_2 ratios as
 27 well as the v_2 - $[p_T]$ correlations in isobar collisions [2, 3]. Strange and multi-strange
 28 hadrons have a smaller hadronic cross-section compared to light hadrons, making
 29 their elliptic flow an excellent probe for understanding the initial state anisotropies
 30 of these isobar collisions.

31 **2 Analysis details**

32 In these proceedings, we report strange and multi-strange hadron v_2 in $^{96}\text{Ru}+^{96}\text{Ru}$
 33 and $^{96}\text{Zr}+^{96}\text{Zr}$ collisions at $\sqrt{s_{\text{NN}}} = 200$ GeV using the data collected by the STAR
 34 experiment. A total of nearly 650M events have been analysed for each of the isobar
 35 collisions. The Time Projection Chamber (TPC) and Time-Of-Flight (TOF) have
 36 been used to identify the decay daughters of these shortly lived particles and their
 37 reconstruction. The weakly decaying neutral strange particles K_s^0 and $\Lambda(\bar{\Lambda})$ are recon-
 38 structed using invariant mass technique and their weak-decay (V0) topology through
 39 the decay channel: $K_s^0 \rightarrow \pi^+ + \pi^-$ and $\Lambda \rightarrow p + \pi^-$, respectively [4]. ϕ -mesons have
 40 been reconstructed using the invariant mass technique through its hadronic decay
 41 channel: $\phi \rightarrow K^+K^-$. Event mixing technique is used for combinatorial background
 42 estimation for ϕ meson. The reconstruction of multi-strange particle $\Xi^-(\bar{\Xi}^+)$ involves
 43 finding two secondary vertices and the various topological selections. The combina-
 44 torial background for the weakly decaying particles is constructed using rotational
 45 background method [5]. The η -sub event plane method has been used to calculate
 46 v_2 of these (multi-)strange hadrons [4]. The maximum resolution achieved for the
 47 second order event plane is nearly 48% for both collision systems.

48 **3 Results**

49 Figure 1 shows the v_2 of strange and multi-strange hadrons as a function of p_T for
 50 minimum bias Ru+Ru and Zr+Zr collisions at $\sqrt{s_{\text{NN}}} = 200$ GeV. An approximate
 51 mass ordering at low p_T and a baryon-meson splitting at intermediate p_T is observed.
 52 All particles and anti-particles tend to follow the number of constituent quark (NCQ)

53 scaling within 10% as shown in Fig. 1, indicating partonic collectivity as well as dom-
 54 ination of quark coalescence mechanism for hadronization at intermediate p_T region.
 A clear centrality dependence of v_2 has been observed for K_s^0 , Λ and Ξ^- as shown in

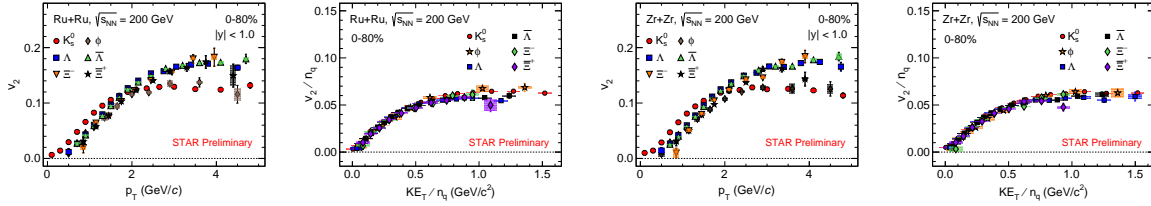


Figure 1: v_2 as a function of p_T of (multi-)strange hadrons and NCQ-scaled v_2 as a function of transverse kinetic energy for Ru+Ru and Zr+Zr collisions at $\sqrt{s_{NN}} = 200$ GeV. The vertical lines and shaded boxes denote statistical and systematic uncertainties, respectively.

55

Fig. 2 and for other hadrons for the isobar collision systems. The p_T -integrated v_2 for

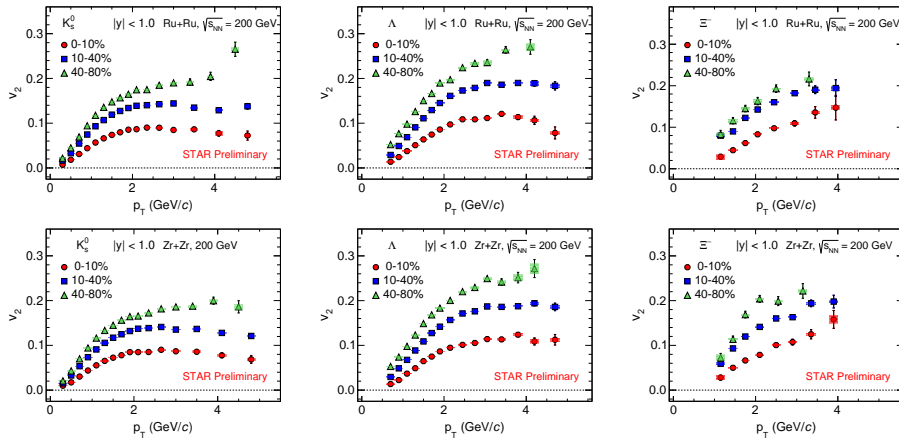


Figure 2: Top panel: Centrality dependence of v_2 of K_s^0 , Λ and Ξ^- as a function of p_T in Ru+Ru collisions at $\sqrt{s_{NN}} = 200$ GeV; Bottom Panel: Same for Zr+Zr collisions at $\sqrt{s_{NN}} = 200$ GeV. The vertical lines and shaded boxes denote statistical and systematic uncertainties, respectively.

56

57 strange hadrons was also studied as a function of the collision centrality as shown in
 58 Fig. 3. The ratios of v_2 between the two isobar collisions for K_s^0 , Λ , and $\bar{\Lambda}$ show clear
 59 deviation of nearly 2% from unity in mid-central collisions, indicating a difference in
 60 nuclear structure and shape [1].

61 We investigated the system size evolution of v_2 by comparing the $^{63}_{29}\text{Cu}+^{63}_{29}\text{Cu}$,
 62 $^{96}_{44}\text{Ru}+^{96}_{44}\text{Ru}$, $^{96}_{40}\text{Zr}+^{96}_{40}\text{Zr}$, $^{197}_{79}\text{Au}+^{197}_{79}\text{Au}$ collisions in 0-80% centrality at $\sqrt{s_{NN}} = 200$
 63 GeV, and $^{238}_{92}\text{U}+^{238}_{92}\text{U}$ collisions at $\sqrt{s_{NN}} = 193$ GeV [6–8]. Figure 4 shows an approx-
 64 imate system size dependence of v_2 for $p_T > 1.8$ GeV/ c , based on the nuclear size.

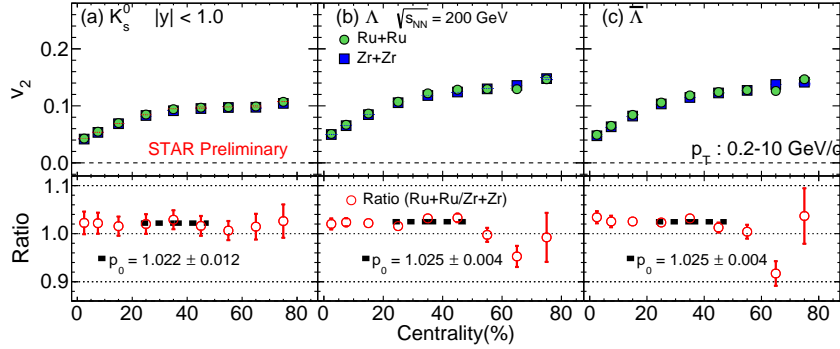


Figure 3: p_T -integrated v_2 as a function of centrality for K_s^0 , Λ , and $\bar{\Lambda}$ in Ru+Ru and Zr+Zr collisions at $\sqrt{s_{NN}} = 200$ GeV. The vertical lines on the ratio includes statistical and systematic uncertainties. The dotted lines denotes the fitting with a constant.

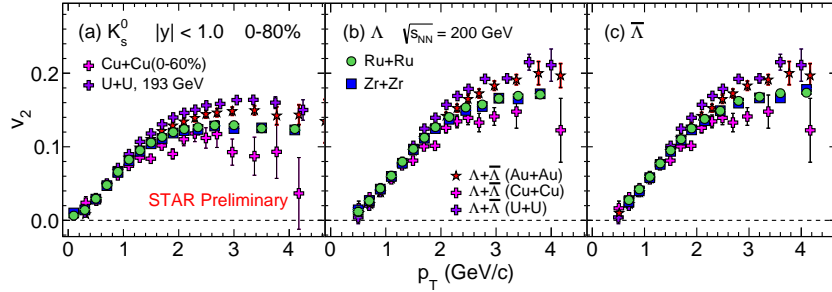


Figure 4: v_2 of K_s^0 , Λ and $\bar{\Lambda}$ in minimum bias Cu+Cu, Ru+Ru, Zr+Zr, Au+Au collisions at $\sqrt{s_{NN}} = 200$ GeV and U+U collisions at $\sqrt{s_{NN}} = 193$ GeV [6–8].

65 The v_2 in U+U and Au+Au is observed to be higher, whereas in Cu+Cu is slightly
 66 lower than those in isobar collisions.

67 4 Conclusion

68 In conclusion, we presented the elliptic flow of K_s^0 , Λ , $\bar{\Lambda}$, ϕ , Ξ^- , and $\bar{\Xi}^+$ particles in
 69 Ru+Ru and Zr+Zr collisions at $\sqrt{s_{NN}} = 200$ GeV. In both isobar species, we noticed a
 70 mass ordering at low p_T and a baryon-meson splitting at intermediate p_T . The NCQ
 71 scaling, which is representative of the partonic degrees of freedom and coalescence
 72 hadronization, is followed by all strange particles and anti-particles. The hadron v_2
 73 ratio exhibits a deviation from unity of around 2% when integrated over p_T . This
 74 indicates the differences in nuclear density and deformation between the two isobar
 75 nuclei. On comparing several collision systems with comparable beam energies, we
 76 also observed the v_2 to be higher for larger colliding systems.

References

1. Abdallah MS, Aboona BE, Adam J, et al., (STAR Collaboration). Search for the chiral magnetic effect with isobar collisions at $\sqrt{s_{NN}} = 200$ GeV by the STAR Collaboration at the BNL Relativistic Heavy Ion Collider. Phys. Rev. C 2022;105:014901.
2. Zhang C and Jia J. Evidence of Quadrupole and Octupole Deformations in $^{96}\text{Zr} + ^{96}\text{Zr}$ and $^{96}\text{Ru} + ^{96}\text{Ru}$ Collisions at Ultrarelativistic Energies. Phys. Rev. Lett. 2022;128:022301.
3. Jia J, Huang S, and Zhang C. Probing nuclear quadrupole deformation from correlation of elliptic flow and transverse momentum in heavy ion collisions. Phys. Rev. C 2022;105:014906.
4. Adamczyk L, Adkins JK, Agakishiev G, et al., (STAR Collaboration). Elliptic flow of identified hadrons in Au+Au collisions at $\sqrt{s_{NN}} = 7.7\text{--}62.4$ GeV. Phys. Rev. C 2013;88:014902.
5. Adams J, Aggarwal MM, Ahammed Z, et al., (STAR Collaboration). Multistrange Baryon Elliptic Flow in Au + Au Collisions at $\sqrt{s_{NN}} = 200$ GeV. Phys. Rev. Lett. 2005;95:122301.
6. Abelev BI, Aggarwal MM, Ahammed Z, et al., (STAR Collaboration). Charged and strange hadron elliptic flow in Cu + Cu collisions at $\sqrt{s_{NN}} = 62.4$ and 200 GeV. Phys. Rev. C 4 2010;81:044902.
7. Abelev BI, Aggarwal MM, Ahammed Z, et al., (STAR Collaboration). Centrality dependence of charged hadron and strange hadron elliptic flow from $\sqrt{s_{NN}} = 200$ GeV Au+Au collisions. Phys. Rev. C 2008;77:054901.
8. Abdallah MS, Adam J, Adamczyk L, et al., (STAR Collaboration). Azimuthal anisotropy measurements of strange and multistrange hadrons in U + U collisions at $\sqrt{s_{NN}} = 193$ GeV at the BNL Relativistic Heavy Ion Collider. Phys. Rev. C 2021;103:064907.